Journal of Alloys and Compounds 480 (2009) 717–722

Contents lists available at ScienceDirect

Journal of Alloys and Compounds

journal homepage: www.elsevier.com/locate/jallcom

Optical properties and critical points in ordered $Be_xZn_{1-x}Se$ alloys

S. Kumar[a,*], Tarun K. Maurya[a], S. Auluck[b]

[a] Applied Physics Department, Institute of Engineering and Technology, M. J. P. Rohilkhand University, Bareilly-243 006, U.P., India
[b] Physics Department, Indian Institute of Technology, Kanpur-208 016, U.P., India

ARTICLE INFO

Article history:
Received 26 September 2008
Received in revised form 5 February 2009
Accepted 10 February 2009
Available online 28 February 2009

Keywords:
Semiconductors
Electronic properties
Optical properties
Computer simulations

ABSTRACT

We have investigated the electronic and optical properties of ordered $Be_xZn_{1-x}Se$ alloys using a 8-atom supercell for compositions $x = 0.0, 0.25, 0.50, 0.75$ and 1.0. We report '*state-of-the-art*' calculations within generalized gradient approximation (GGA) and Engel-Vosko's corrected generalized gradient approximation (EVGGA) using the full potential linear augmented plane wave (FPLAPW) method as implemented in the WIEN2K code. To see the effect of disorder, alloys are also modeled following the special quasirandom structure (SQS) approach. The calculated lattice constants scale linearly with composition (Vegard's law). Dielectric functions for different compositional alloys are calculated for 8-atom cubic supercell and chalcopyrite structure corresponding to [0 0 1] superlattice which show good qualitative agreement when compared with experiment. The calculated band gaps are fitted with a quadratic equation $E_g(x) = ax^2 + bx + c$. We find that there is a direct to indirect band gap crossover at $x = 0.53$ compared with the measured value $x = 0.46$. The position of critical points (CP's) $E_0 + \Delta_0$, E_1 and E_2 show good agreement with the experimental data. The difference between the calculated band gap and measured band gap decreases with increasing concentration of Be. The valence band maxima and conduction band minima are dominated by Se-3p and Zn-4s/Be-2p states for $x = 0.0$ and 1.0, respectively.

1. Introduction

In the last few years dedicated efforts have been made to understand the II-VI compounds due to their potential applications as optoelectronic devices while Be based semiconductor compounds and its alloys are comparatively less studied due to their high toxic nature. Addition of Be in II-VI compounds like ZnSe and ZnTe would lead to better device properties of the II-VI compounds. Waag et al. [1] have suggested doping of Be in ZnSe (BeZnSe alloys) results in improved hardness [2,3] and a longer life time of the devices. Smaller concentrations of Be are required to obtain larger band gaps and have a lattice matched with GaAs [4]. The large band gap of BeSe (5.15 eV) suggests the possibility of using these materials for ultraviolet (UV) optoelectronic applications. Chauvet et al. [5] have grown $Be_xZn_{1-x}Se$ alloys on a GaAs substrate by molecular beam epitaxy (MBE) [6] and studied reflectivity to locate direct to indirect band gap crossover. Wilmers et al. [7] have grown $Be_xZn_{1-x}Se$ layers on a GaAs substrate by MBE and measured the dielectric functions for the full composition range (i.e. $x = 0.0$ to 1.0) by ellipsometric spectroscopy. As far as the theoretical calculations are concerned, the emphasis has been on the electronic and structural properties. Stukel [8] performed theoretical calculations for electronic and optical properties of BeX (X=Te, Se, S) compounds. Grein et al. [9] had used virtual crystal approximation (VCA) within density functional theory (DFT) to find the direct to indirect crossover in $Zn_xBe_{1-x}Se$ alloys. Postinikov et al. [10] have calculated the vibrational properties using SIESTA (Spanish Initiative for Electronic Simulations with Thousands of Atoms) code [11] with norm-conserving pseudopotential and localized basis function. Ground state properties and structural phase transitions for BeX were studied by Hassan and Akberzadeh [12]. Baaziz et al. [13] have calculated the composition dependent structural and electronic properties of $Be_xZn_{1-x}Se$ alloys. Ameri et al. [14] have used full potential linear muffin tin orbital (FP-LMTO) method to see the effect of Be doping in ZnSe on structural properties. Berghout et al. [15] have used plane wave pseudopotential scheme to study the thermodynamical problem of $Zn_{1-x}Be_xSe$ alloys. Recently Kumar et. al. [16] have studied the electronic and optical properties of $Be_xZn_{1-x}Se$ alloys by using the full potential linear augmented plane wave method (FPLAPW) [17]. Bouhafs and co-workers [18] have studied structural properties of Pb-based alloys using hybrid FPLAPW method. In this paper we extend our previous work [16] to the discussion of the critical points.

A brief description of the computational details and methodology are given in Section 2. We present the theoretical results in Section 3. Concluding remarks are presented at the end of the paper.

* Corresponding author: Tel.: +91 581 2524232
E-mail address: drsudhirkumar.in@gmail.com (S. Kumar).

0925-8388/$ – see front matter.
doi:10.1016/j.jallcom.2009.02.051

2. Computational methods

The computational method is based on a scalar relativistic, full potential linearized augmented plane wave method (FPLAPW) [17] as implemented in the WIEN2K code [19] which is known to give precise energy eigenvalues and eigenfunctions. Density functional calculations can be divided into two classes. The first one uses pseudopotentials with a relatively simple basis set and the other methods use a more complex basis set. The later class fall the full potential linearized augmented plane wave (FPLAPW) and linearized muffin tin orbital (FPLMTO) methods. However both approaches have a common plane wave basis set. Spherical and non-spherical potentials are treated separately in the FPLAPW method contrary to LMTO [20] method in which a muffin potential is taken into account. In the FPLAPW method the basis set is obtained by dividing the unit cell into non-overlapping atomic spheres (centered on the atomic sites) and an interstitial region. The atomic sphere radii are chosen to be 1.8, 2.0 and 2.1 atomic unit (a.u.) for Be, Zn and Se respectively. In the muffin-tin (MT) spheres, the l-expansion of the non-spherical potential and charge density was carried out up to $l_{max} = 10$. In order to achieve energy eigenvalue convergence, the basis function is expanded up to $R_{MT}K_{max} = 7.0$ (where K_{max} is the maximum modulus for the reciprocal lattice vector and R_{MT} is the average radius of the MT sphere). In order to see the convergence of the wave functions, we have also checked our results by taking the value of $R_{MT}K_{max} = 9.0$. Our results were remains unchanged or very minor changed. The exchange correlation potential is treated within the generalized gradient approximation (GGA) [21] and Engel-Vosko's GGA (EVGGA) [22]. It is known that both local density approximation (LDA) and GGA usually underestimates the band gap. This underestimation of the band gap is due to the fact that they have the simple forms and are not sufficiently flexible to reproduce both the exchange correlation energy and its derivative accurately. Engel and Vosko [22] considered this shortcoming and constructed a new functional form of GGA which is able to better reproduce the exchange potential at the expense of less agreement in exchange energy. This approach which is called EVGGA, yields a better band splitting and some other properties which mainly depend on the accuracy of exchange correlation potential.

The self consistency was obtained by using 216 k-points in the irreducible Brillouin zone (IBZ). The Brillouin zone integrations were carried out using the tetrahedron method [23]. Since calculations of the optical properties require a more dense k-space matrix, we use 512 k-points for the calculations of the dielectric functions. In this work, we have modeled the ordered alloy by considering a 8-atom cubic supercell as well as chalcopyrite (CH) structure which is a superlattice along [0 0 1] following the SQS approach [24]. The 8-atom cubic supercell consist of four atoms of Zn and four atoms of Se. For $x = 0.25$, we replace one Zn atom at the corner with Be and for $x = 0.75$ we replace three corner atoms of Zn by Be. Thus, we are using the simple $Li_0$and Li_2 structures. It is obvious that there are other options also. We find that for $x = 0.50$, the alloy has a layered structure. We consider alternate layers of Zn and Be atoms along [0 0 1] direction sandwiched between two layers of Se atoms. This gives a cubic unit supercell along [0 0 1] direction. We would like to mention that our calculations are for ordered alloys while the experimental data is for disordered alloys. This requires that we should follow the special quasirandom structure (SQS) approach [24]. In this case the 8-atom CH layered structure is a short period superlattice whose layers are stacked in a standard orientation i.e. [0 0 1]. In practice, the layer stacking in SQS are chosen in non-standard directions e.g. [1 1 3], [3 3 1], [1 1 5]. We hope to look into such type of structures in future. The usefulness of these SQS semiconductor alloys are discussed by Wei and Zunger [24]. As a matter of fact, we have taken the first step to make a separate calculation of the dielectric function for $x = 0.25$, 0.50 and 0.75 following the SQS approach. We have replaced Zn atoms by Be to get required concentration of Be as follows: To get 25% and 75% concentration of Be, one corner atom of Zn and one corner atom alongwith two face atoms of Zn are replaced by Be. To get 50% of Be concentration two atoms of Zn are replaced by Be. It is true that there other arrangements are also possible. We have checked the difference in calculated optical properties for two different arrangements of Be atoms in $Be_{0.50}Zn_{0.50}Se$ alloy. There is no significant difference between two different arrangements which is not presented here. The detailed formulation for the determination of the linear dielectric function (tensor) $\varepsilon(\omega) = \varepsilon_1(\omega) + i\varepsilon_2(\omega)$ with the FP-LAPW method has been discussed by Draxl and Sofo [25]. For cubic structure, principal component of $\varepsilon_2(\omega)$ are equal, i.e. $\varepsilon_2^{xx}(\omega) = \varepsilon_2^{yy}(\omega) = \varepsilon_2^{zz}(\omega)$. However, for the CH structure, the principal component of $\varepsilon_2^{zz}(\omega)$ are not equal to $\varepsilon_2^{xx}(\omega)$, i.e. $\varepsilon_2^{xx}(\omega) = \varepsilon_2^{yy}(\omega) \neq \varepsilon_2^{zz}(\omega)$ which shows anisotropy in $\varepsilon_2(\omega)$. This is due to the choice of the co-ordinate system. In the CH system the x-axis does not show a four fold rotation symmetry as in the cubic structure. Therefore, we calculate the average $\varepsilon_2(\omega)$ spectra for CH structure using $\varepsilon_2(\omega) = [2\varepsilon_2^{xx}(\omega) + 2\varepsilon_2^{yy}(\omega) + \varepsilon_2^{zz}(\omega)]/3$ to compare with the cubic spectrum. The optical response is calculated by the standard expresion for $\varepsilon_2(\omega)$ [26]

$$\varepsilon_2(\omega) = \left(\frac{4\pi e^2}{m^2\omega^2}\right)\sum_{ij}\int |\langle i|M|j\rangle|^2 f_i(1-f_j)\delta(E_f - E_i - \omega)d^3k \qquad (1)$$

where M is the dipole operator, i and j are the initial and final states respectively, f_i is the Fermi distribution function for the ith state, E_i is the energy of electron in the ith state.

3. Results and discussion

3.1. Structural parameters

The structural parameters of $Be_xZn_{1-x}Se$ alloys are computed for the five different compositions of $x = 0.0$, 0.25, 0.50, 0.75 and 1.0. The results of structural optimization of $Be_xZn_{1-x}Se$ alloys are presented elsewhere [16]. In Fig. 1, we present our calculated lattice constants as a function of beryllium concentration alongwith with Vegard's law and SIESTA [10] results. The lattice constant scales linearly with composition thus obeying Vegard's law. Our results show a maximum deviation of 1.7% for $x = 0.25$. However, it is well known that GGA overestimates the lattice constants and such a small differences are expected [16]. We have calculated the bulk modulus using the Murnaghan's equation of state [27]. The calculated bulk modulus for ZnSe and BeSe are compared with measured data [28,29]

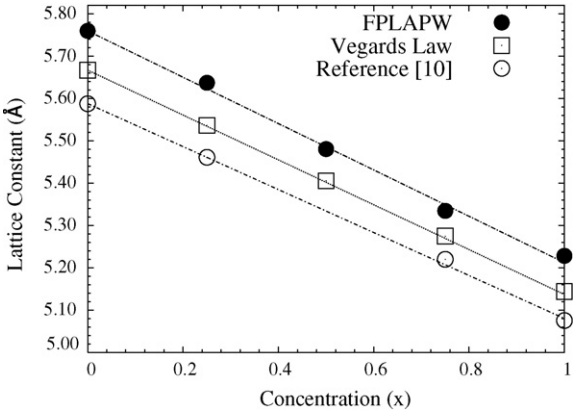

Fig. 1. Calculated equilibrium lattice constants of $Be_xZn_{1-x}Se$ alloys with filled circles alongwith SIESTA results Ref. [10](open circles) and Vegard's law Ref. [37,41](open squares) are shown.

Table 1
Bulk modulus of $Be_xZn_{1-x}Se$ alloys.

System	Lattice constant [present calculation]	B_0 (GPa)	B_0 [experimental]	Other calculation
ZnSe	5.7598 (5.667)	63.8256	62.5 [a]	56.826 [c]
$Be_{0.25}Zn_{0.75}Se$	5.6371	64.4782	–	60.810 [c]
$Be_{0.50}Zn_{0.50}Se$	5.4805	65.9804	–	65.407 [c]
$Be_{0.75}Zn_{0.25}Se$	5.3346	70.3573	–	70.136 [c]
BeSe	5.2282 (5.144)	83.8723	92.2 [b]	74.569 [c]

[a] Ref. [28].
[b] Ref. [29].
[c] Ref. [13].

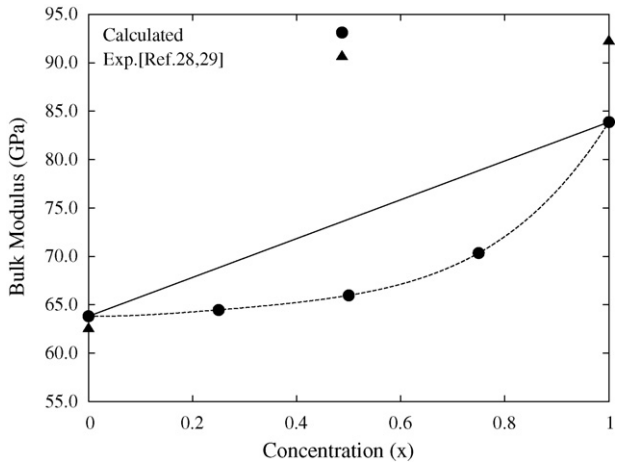

Fig. 2. Calculated Bulk moduli, for $Be_xZn_{1-x}Se$ alloys for five different concentrations i.e. $x = 0.0, 0.25, 0.50, 0.75$ and 1.0. Measured values are taken from Ref. [28,29].

presented in Table 1 and Fig. 2 shows good agreement and better than previous calculations [13].

3.2. Band gap crossover

The calculated energy band gaps for cubic supercell of $Be_xZn_{1-x}Se$ alloys are presented in Table 2. For the CH structure, we found relatively smaller band gaps in contrast to the cubic supercell. This is in agreement with the previous calculations [30] which predicts that SQS show a little smaller band gap. The major drawback of density functional theory in calculating band gaps lies in the exchange correlation term. To see the effect of exchange correlation, we have compared band gaps calculated with GGA (EVGGA)

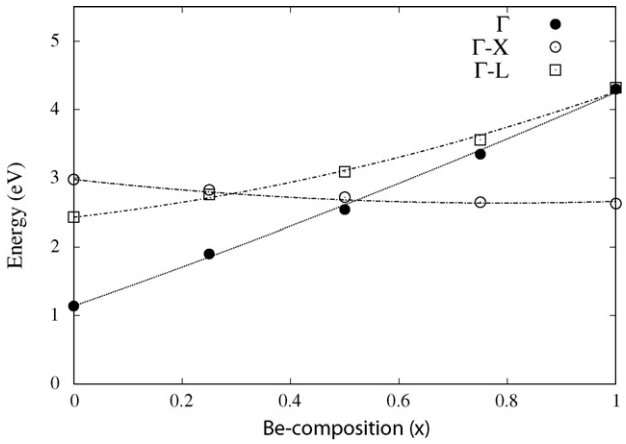

Fig. 3. The variation of band gap (eV) with concentration x for $Be_xZn_{1-x}Se$ alloys showing cross-over.

presented in Table 2. We find that there is significant improvement in the calculated band gap with the EVGGA exchange correlation potential. On the other hand, in order to get the precise value of the band gap, one has to go for GW approach which needs self energy (Σ), where G = Green's function and W = Coulomb interaction, should be estimated precisely. GW calculation is cumbersome needs heavy computational time which is not considered in the present paper. The detailed band structure calculations and density of states are discussed elsewhere [31]. The energy band gaps variation in different directions ($\Gamma - X$ and $\Gamma - L$) are presented in Fig. 3. Photoluminescence measurements, to locate the direct to indirect band gap crossover in $Be_xZn_{1-x}Se$ alloys, have been carried out by Chauvet et al [5]. This was found to occur at $x = 0.46$ whereas our band gap crossover occurs at $x = 0.53$, see Fig. 3. We have fitted the $\Gamma - L$ and $\Gamma - X$ variations in the composition range ($x = 0.0$ to 1.00) to locate the direct to indirect band gap crossover presented in Fig. 3. The best fit for $\Gamma - X$ and $\Gamma - L$is

$$E_g^{\Gamma-X}(x) = 0.55x^2 - 0.87x + 2.98 \quad (2)$$

$$E_g^{\Gamma-L}(x) = 0.90x^2 + 0.93x + 2.43 \quad (3)$$

The bowing factor is equal to 0.55 and 0.90 eV along $\Gamma - X$ and $\Gamma - L$ respectively. It should be noted that composition x dependent band gaps bowing are different along different symmetry direction. The location of direct $\Gamma - L$ to $\Gamma - X$ band gap cross over does not depend on the absolute value of the energy gap instead it depends on the relative changes in band gap i.e. slope

Table 2
Calculated band gaps for $Be_xZn_{1-x}Se$ alloys along differnt line in k-space under GGA (EVGGA) scheme (all in eV).

System	Present calculation			Previous study	Experimental	
	$(\Gamma - \Gamma)$	$(\Gamma - X)$	$(\Gamma - L)$	$(\Gamma - \Gamma)$	$(\Gamma - \Gamma)$	$(\Gamma - X)$
ZnSe	1.14 (1.99)	2.98 (3.90)	2.43 (3.08)	1.04 [a], 2.41 [b], 2.69 [b], 1.11 [c]	2.58 [d]	–
$Be_{0.25}Zn_{0.75}Se$	1.90 (2.65)	2.83 (3.75)	2.76 (3.35)	1.64 [c]	3.5 [e]	–
$Be_{0.50}Zn_{0.50}Se$	2.54 (3.42)	2.72 (4.22)	3.09 (3.71)	2.27 [c]	3.95 [e]	–
$Be_{0.75}Zn_{0.25}Se$	3.35 (3.59)	2.65 (4.25)	3.56 (4.13)	2.75 [c]	4.4 [e]	–
BeSe	4.30 (4.79)	2.63 (3.62)	4.32 (4.93)	4.37 [f], 5.47 [g], 4.72 [h], 4.19 [c]	5.55 [i]	4.0 [j]

[a] Ref. [40].
[b] Ref. [42].
[c] Ref. [13].
[d] Ref [32].
[e] Ref [5] for $Be_{0.67}Zn_{0.33}Se$.
[f] Ref. [39].
[g] Ref. [41].
[h] Ref. [38].
[i] Ref. [7].
[j] Ref. [43].

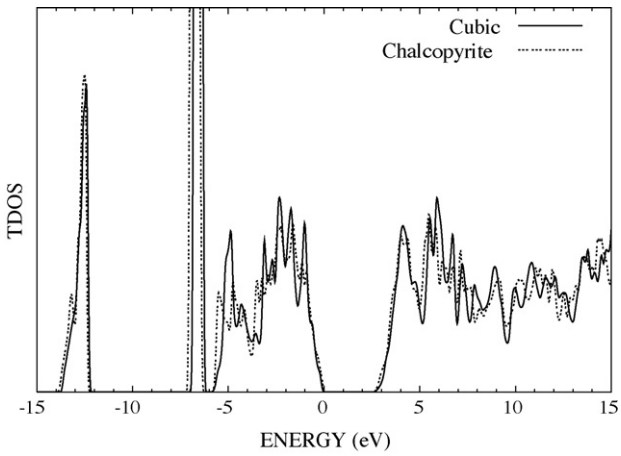

Fig. 4. The total density of states of $Be_xZn_{1-x}Se$ alloys for $x = 0.50$ for cubic and CH structure.

of the fitted curve. Therefore, our estimated value of crossover is unaffected even though GGA/EVGGA underestimates the band gaps.

3.3. Cubic and chalcopyrite structure

In this section, we mainly focus our attention to the comparison of the calculated response function and density of states (DOS) for cubic and CH structure at the cell volume 1064.0974 a.u.^{3}and 1066.9413 a.u.^{3} respectively for $Be_{0.50}Zn_{0.50}Se$. In Fig. 4, we present calculated total density of states for CH and cubic structure for $Be_{0.50}Zn_{0.50}Se$. The projected density of states (PDOS) for cubic is presented and discussed elsewhere [16]. The total DOS for CH structure is shifted towards lower energy ≈ 0.1 eV and show more structure than the cubic case. This is due to the fact that CH is a layered structure which takes account the disorder effect better than the simple cubic or Li_0/Li_2structure.

4. Optical properties

The calculation of $\varepsilon_2(\omega)$ requires energy eigenvalues and electron wavefunctions. These are natural outputs of the band structure calculations. In this section, we present calculations for $\varepsilon_2(\omega)$ and compare them with available experimental data [7]. In Fig. 5, the calculated $\varepsilon_2(\omega)$ are presented for $Be_xZn_{1-x}Se$ alloys for cubic (CH) structure for different concentrations, i.e. $x = 0.0$, 0.25 (0.25), 0.50 (0.50), 0.75 (0.75), and 1.0 along with the measured [7] dielectric functions for $x = 0.0$, 0.30, 0.50, 0.70 and 1.0 concentrations respectively. As mentioned earlier, care should be excerised when comparing the two because the theoretical calculations are for ordered alloys while the experimental data's for disordered alloys.

The Gaussian broadening parameter is taken to be 0.1 eV. The calculated $\varepsilon_2(\omega)$ of cubic (CH) structure of $Be_xZn_{1-x}Se$ alloys for five concentrations $x = 0.0$, 0.25 (0.25), 0.50 (0.50), 0.75 (0.75), and 1.00 are shifted by 0.90, 0.510 (0.51), 0.310 (0.451), 0.150 (0.304), 0.175 eV, respectively, by using the scissor operator shift (SOS). We shift the calculated spectrum by the SOS rigidly so as to match the onset of $\varepsilon_2(\omega)$ and CP's with the measured spectrum. The value of SOS in CH structure are little larger because calculated band gap is smaller in SQS structure as discussed in Section 3.2. It would be interesting to find the SOS for the end compounds and then use interpolation. However the SOS does not follow Vegard's law. The calculated E_g for ZnSe and BeSe are 55.5% and 22.5% lower than the experimental values [7,32]. Accordingly the value of the SOS for BeSe is approximately equal to one third that of ZnSe. We have not used the SOS in calculating the band crossover.

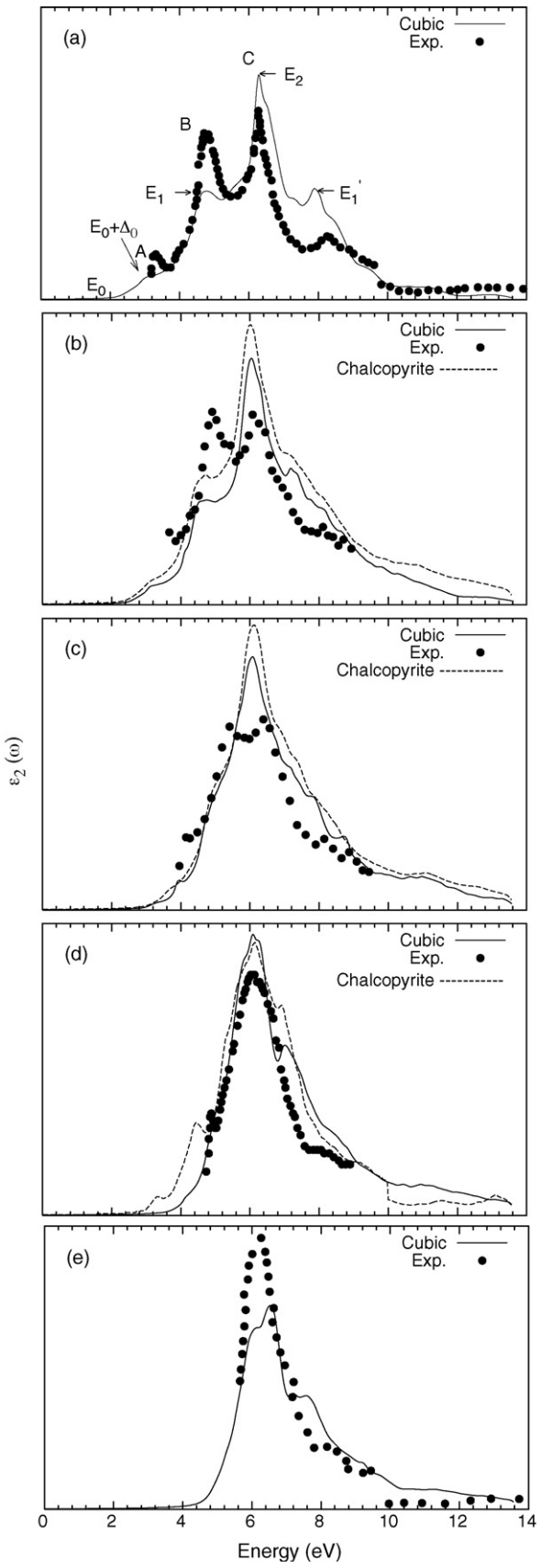

Fig. 5. Calculated $\varepsilon_2(\omega)$, for $Be_xZn_{1-x}Se$ alloys for five different concentrations i.e. $x = 0.0$, 0.25, 0.50, 0.75 and 1.0. Measured values of $\varepsilon_2(\omega)$ are shown by dark circles and taken from Ref. [7].

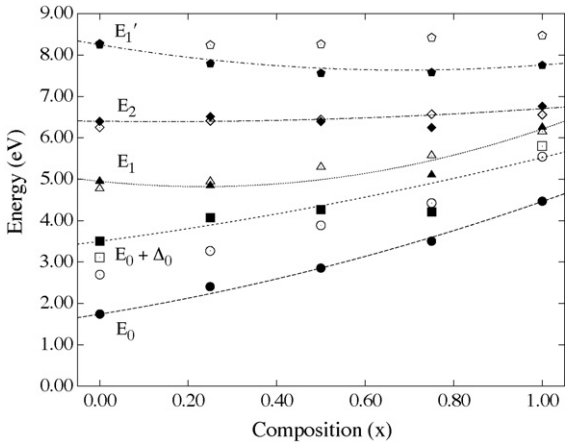

Fig. 6. The critical energies of the calculated structures for $Be_xZn_{1-x}Se$ alloys as a function of the beryllium composition. The obtained critical points E_0, $E_0 + \Delta_0$, E_1, E_2 and E_1' are shown by filled symbols i.e. circle, square, triangle, diamond and pentagon respectively while corresponding experimental critical points Ref. [7] are shown by empty symbols.

For the cubic supercell our calculated $\varepsilon_2(\omega)$ for ZnSe i.e. $x = 0.0$ is consistent with the earlier calculations performed by Walter et al. [33] and Kim and Sivananthan [34]. The calculated $\varepsilon_2(\omega)$ for $x = 0.0$ presented in Fig. 5 a. has a small peak at 2.6 eV. This could be due to transitions from occupied Se-p states to the unoccupied Zn-s state of the conduction band. The sharp rise in $\varepsilon_2(\omega)$ at 4.0 eV reaches a maxima at 4.5 eV. This maxima arises from transitions just below E_F i.e. Se-p and Se-d states to just above it i.e. Zn-s and Se-p states. The main structure at 6.0 eV is dominated by the transitions from Se-p and Zn-d states (4.0 eV to 6.7 eV) below E_F to the Se-p and Zn-p states (3.0 eV) above E_F. We note that with increasing Be concentration x the conduction band minima moves towards higher energies. This causes the structures at 2.6 eV and 4.5 eV to move towards higher energies and finally merge with the main structure at 6.2 eV for BeSe. The shifting of the peaks with increasing x is consistent with PL data [5]. With the increasing Be concentrations the conduction band states change from Se-p and Zn-p to Be-s,p states. We have mentioned different critical points (CP's) in the inset. The CP's E_0 and $E_0 + \Delta_0$ arise from transitions at the centre of the Brillouin zone. The E_1 CP arises from transitions along the [1 1 1] directions and the E_2 CP from [1 1 0] direction.

The averaged $\varepsilon_2(\omega)$ for CH structure for $x = 0.25$, 0.50 and 0.75 are presented in Fig. 5 to compare with the cubic structure. The averaged $\varepsilon_2(\omega)$ for CH does not show any significant differences from cubic except for $Be_{0.75}Zn_{0.25}Se$ alloys. The structure at 4.45 eV compares well with the experimental structure at 4.76 eV. This structure may correspond to transition between the parallel valance bands and first conduction band around P-point of the CH structure presented elsewhere [31].

The position of the CP's for cubic structure, extracted from the calculated $\varepsilon_2(\omega)$ spectra are presented in Fig. 6. alongwith the experimental data [7]. The E_2 and $E_0 + \Delta_0$ CP's are fitted with linear equations while the other CP's (E_0, E_1 and E_1') are fitted with quadratic equations. There is overall good agreement with experiment. However the E_0 and E_1' experimental data's are not lie on the fitted curve. This could be due to the uncertainty in locating the positions of the CP's. The fitting parameters are presented in Table 3.

The measurements have been done for the disordered samples while our calculations are for ordered alloys. It is known that disorder leads to the increase the possibility of indirect optical transitions and violates translational symmetry. We find reasonable agreement with the experimental data for alloys in contrast to ZnSe.

Table 3
Composition (x) dependence of the parameters approximated by the quadratic equation $E(x) = ax^2 + bx + c$ for critical points E_0, $E_0 + \Delta_0$, E_1 and E_2 and E_1' (all in eV).

	E_0	$E_0 + \Delta_0$	E_1	E_2	E_1'
a	0.99	0.612	2.367	0.4215	1.29
b	1.73	1.411	−1.103	−0.115	1.78
c	1.74	3.50	4.95	6.40	8.25

This suggests that effect of disorder may not be large. In the measured spectra of ZnSe the second structure at 4.5 eV could be due to excitonic effects [35,36]. Excitonic effects are not included in the present calculation. A similar problem with Si optical spectra has been discussed and solved satisfactorily by Sottile [37] taking into account excitonic effects.

5. Conclusions

Our calculated values of the bulk moduli are in better agreement with the measured data compared to previous calculations. The obtained direct to indirect crossover ($\Gamma - X$) shows good agreement with measured data. This is due to the fact that crossover depends on the relative band gap energy instead of absolute value. We are able to get trends of $\varepsilon_2(\omega)$ that are in agreement with the experimental data. The position of CP's $E_0 + \Delta_0$, E_1 and E_2 are in good agreement with the measured data. We would like to stress that our calculations with cubic and CH structures are able to explain most of the experimental structure. In spite of simplifications, the agreement with an experimental data is very encouraging.

Acknowledgments

One of us (S. Kumar) is thankful to the Department of Science and Technology and University Grants Commission, New Delhi for their financial support.

References

[1] A. Waag, Th. Litz, F. Fisher, H.-J. Lugauer, T. Baron, K. Schull, U. Zehnder, T. Gerhard, U. Lunz, M. Keim, G. Reuscher, G. Landwehr, J. Cryst. Growth 184/185 (1998) 1.
[2] C. Verie, J. Cryst. Growth 184/185 (1998) 1061.
[3] K. Maruyama, K. Suto, J.I. Nishizawa, J. Cryst. Growth 214/215 (2000) 104.
[4] V. Bousquet, E. Tournie, M. Laogt, P. Vennegus, J.P. Faurie, Appl. Phys. Lett. 70 (1997) 3564–3566.
[5] C. Chauvet, E. Tournié, J.P. Faurie, Phys. Rev. B 61 (2000) 5332.
[6] S.P. Guo, Y. Luo, W. Lin, O. Maksimov, M.C. Tamargo, I. Kuskovsky, C. Tian, G.F. Neumark, J. Cryst. Growth 208 (2000) 205.
[7] K. Wilmers, T. Wethkamp, N. Esser, C. Cobet, W. Richter, M. Cardona, V. Wagner, H. Lugauer, F. Fischer, T. Gerhard, M. Keim, Phys. Rev. B 59 (1999) 10071.
[8] D.J. Stukel, Phys. Rev. B 2 (1970) 1852.
[9] C.H. Grein, R.J. Radtke, H. Ehrenreich, C. Chauvet, E. Tournie, J.P. Faurie, Solid State Commun. 123 (2002) 209–212.
[10] A.V. Postnikov, O. Pagés, J. Huggel, Phys. Rev. B 71 (2005) 115206.
[11] J.M. Soler, E. Artacho, J.D. Gale, A. García, J. Junquera, P. Ordejón, D. Sánchez-Portal, J. Phys. Condens. Matter. 14 (2002) 2745.
[12] F. El Haj Hassan, H. Akbarzadeh, Comput. Mater. Sci. 53 (2006) 423.
[13] H. Baaziz, Z. Charifi, F. El Haj Hassan, S.J. Hashemifar, H. Akbarzadeh, Phys. Status Solidi (b) 243 (6) (2006) 1296–1305.
[14] M. Ameri, D. Rached, M. Rabah, R. Khenata, N. Benkhettou, B. Bouhafs, M. Maachou, Mater. Sci. Semicond. Process 10 (2007) 6–13.
[15] A. Berghout, A. Zaoui, J. Hugel, M. Ferhat, Phys. Rev. B 75 (2007) 205112.
[16] S. Kumar, T.K. Maurya, S. Auluck, J. Phys. Condens. Matter 20 (2008) 75205.
[17] D.J. Singh, Planewaves Pseudopotentials and the LAPW method, Kluwer Academic, Boston, 1994.
[18] A. Zaoui, S. Kacimi, M. Zaoui, B. Bouhafs, Mater. Chem. Phys. (2008), doi:10.1016/j.matchemphys.2008.10.020.
[19] P. Blaha, K. Schwarz, G.K.H. Madson, D. Kvasnica, Comput. Phys. Commun. 59 (1990) 339.
[20] M. Methfessel, Phys. Rev. B 38 (1993) 1537.
[21] J.P. Perdew, S. Burke, M. Ernzerhof, Phys. Rev. Lett. 77 (1996) 3865.
[22] E. Engel, S.H. Vosko, Phys. Rev. B 47 (1993) 13164.
[23] O. Jepson, O.K. Anderson, Solid State Commun. 9 (1971) 1763.
[24] A. Zunger, S.H. Wei, L.G. Ferireira, T.E. Bernard, Phys. Rev. Lett. 65 (1990) 353.
[25] C. Ambrosch-Draxl, J.O. Sofo, Comput. Phys. Comm. 175 (2006) 1.

[26] A.H. Reshak, S. Auluck, Phys. Rev. B 68 (2003) 125101.
[27] F.D. Murnghan, Proc. Natl. Sci. U.S.A. 30 (1944) 244.
[28] O. Madelung, Londolt-Bornstein New Series III, Vol. 22, Springer, Berlin, 1982.
[29] H. Luo, K. Ghandehair, R.G. Geene, A.L. Ruoff, S.S. Trail, F.J. DiSalvo, Phys. Rev. B 52 (1995) 7058.
[30] R. Magri, S. Froyen, A. Zunger, Phys. Rev. B 44 (1991) 7947.
[31] T.K. Maurya, Ph.D Thesis, M. J. P. Rohilkhand University, Bareilly, India, 2008.
[32] R.C. Weast, D.R. Lide, M.J. Astle, W.H. Beyer, CRC Handbook of Chemistry and Physics, 70th ed., Chemical Rubber, Boca Raton, 1990.
[33] J.P. Walter, M.L. Cohen, Y. Petroff, M. Balkanski, Phys. Rev. B 1 (1970) 2661.
[34] C.C. Kim, S. Sivananthan, Phys. Rev. B 53 (1996) 1475.
[35] S. Albrecht, L. Reining, R. Del Sole, G. Onida, Phys. Rev. Lett. 80 (1998) 4510.
[36] L.X. Benedict, E.L. Shirley, R.B. Bohn, Phys. Rev. Lett. 80 (1988) 4514.
[37] F. Sottile, Ph.D Thesis, Private Communication, 2003.
[38] M. González-Diáz, P. Rodríguez-Hernández, A. Munoz, Phys. Rev. B 55 (1997) 14043.
[39] C.M.I. Okoye, Eur. Phys. J. B 39 (2004) 5–17.
[40] B.K. Agrawal, P.S. Yadav, S. Agrawal, Phys. Rev. B 50 (1994) 14881.
[41] A. Fleszar, W. Hanke, Phys. Rev. B 62 (2000) 2466.
[42] W. Luo, S. Ismail-Beigi, M.L. Cohen, S.G. Louie, Phys. Rev. B 66 (2002) 195215.
[43] W.M. Yim, J. Phys. Chem. Solids 33 (1972) 501.